Regular Paper

Performance Analysis of ITS V2V Broadcast Communication Using CSMA/CA and a Roadside Relay Station at Intersections

Huiting Cheng[1,a]   Yasushi Yamao[1,b]

Abstract: The reliability of Carrier Sense Multiple Access with Collision Avoidance (CSMA/CA) vehicle-to-vehicle (V2V) communication in real road environments suffers from fading, shadowing and the hidden terminal problem, especially for non-line-of sight (NLOS) areas such as intersections. In order to improve the communication reliability, a CSMA/CA based vehicle-roadside-vehicle broadcast relay network was proposed and its effectiveness has been shown through simulations. However, the potential of such a network has not been well analyzed and optimized. In this paper, a theoretical model is proposed to analyze the performance of the broadcast relay network in detail. In order to fit real vehicular environments, the model assumes a typical crossroad and takes into account fading, shadowing, the hidden terminal problem and the capture effect. The influence of system parameters including position of nodes, carrier sense threshold and RF frequency band on the reliability of the network is studied based on the model. The accuracy of the proposed analytical model is confirmed by simulations. The analytical model and the obtained results are useful for the design of vehicular broadcast networks to select appropriate system parameters.

Keywords: CSMA/CA, relay network, hidden terminal, capture effect

1. Introduction

Safety and efficiency of transportation are the major objectives of intelligent transportation systems (ITS) applications. Among the active safety applications, one of the promising approaches is vehicle safety communications (VSC)[1], which includes vehicle-to-vehicle (V2V) and vehicle-to-infrastructure (V2I) communications. By exchanging information (such as direction, speed and position) of each vehicle in a broadcast fashion, each vehicle can predict its surrounding vehicles' movements to prevent potential accidents and be aware of the current traffic condition on the road.

Although the reliability of communication is essential in VSC, in real road environments, it suffers from severe attenuation of received signal power due to shadowing and fading, as well as the hidden terminal problem. Especially for intersections in urban area, the corners are often occupied by buildings, which may block the line-of-sight (LOS) path and introduce severe diffraction loss. In order to improve V2V communication performance on intersections, Ref. [2] proposed a vehicle-roadside-vehicle broadcast relay network using Carrier Sense Multiple Access with Collision Avoidance (CSMA/CA) as shown in **Fig. 1**. In this network, a relay station (RS) forwards data packets transmitted by the vehicle stations via broadcasting. The use of RS can mitigate the problems in actual road and extend effectively

the coverage of V2V communications, especially at non-line-of sight (NLOS) areas[3]. However, the performance gain obtained by RS essentially depends on the geometrical position of vehicle stations and the RS. Also, relaying will introduce new collisions between relay transmission and direct V2V communication, which may reduce the performance gain. Those effects have not been investigated previously [2], [3]. Detailed analysis of the performance gain obtained by RS considering those side effects are then necessary to maximize the performance of the relay network.

The packet reception rate performance of CSMA/CA broadcast communications without relay has been analyzed in some works. M. Torrent-Moreno et al. [4] provided extensive and detailed analysis of the characteristics of broadcast transmission consid-
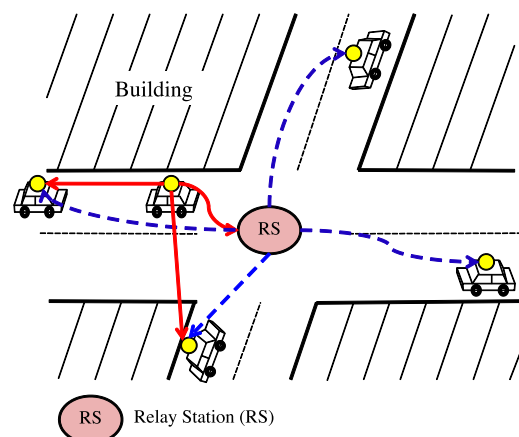
Fig. 1   A vehicle-roadside-vehicle relay communication network.

---

ering different propagation environments via computer simulations. As for theoretical approaches, Ref. [5] analyzed the impact of the hidden terminal problem and distributed coordinate function (DCF) backoff process on packet reception rate. The performance of V2V communications with two safety services of different priorities was evaluated in Ref. [6]. In Ref. [7], the influence of contention window size and number of vehicles has been analyzed and discussed.

However, these theoretical works [5], [6], [7] only considered either non-fading channel or fading channel with a constant bit error rate (BER) regardless of node position. Moreover, they assumed that collision always causes transmission failure, which is not necessarily the case in real wireless environments because of the capture effect [*1]. In Ref. [8], the fading environment and the capture effect were taken into account, which provides more precise packet error analysis. However, it considered neither relaying nor the effect of shadowing in crossroads. The theoretical analysis of the packet reception rate for a broadcast V2V network with relay has not been covered by any pervious works yet.

In this paper, we extend the theoretical model originally proposed by Ref. [8] to analyze CSMA/CA broadcast reception reliability with a RS on an intersection. The proposed model takes into account the fading environment, the hidden terminal problem and the capture effect. Since direct and relayed paths from a transmitting vehicle station (T-VS) to a receiving vehicle station (R-VS) are possible, path diversity effect is also analyzed. Furthermore, we study the impact of position of nodes, carrier sense threshold and RF frequency band on performance in terms of packet reception rate. Our proposed analytical model and obtained observations will give more clear views about how the aforementioned parameters affect the performance, and provide theoretic references in reliable CSMA/CA broadcast network design.

The rest of this paper is organized as follows. Section 2 presents the model for the analysis of packet reception rate in broadcast communication with a relay. The model is applied to an intersection scenario. The validation and discussion of the numerical results are in Section 3. Finally, Section 4 concludes the paper.

2. System Model and Analysis

In this section, the system model of V2V broadcast communication using a roadside RS and the assumptions considered for the analytical model are introduced. Then, the analytical model is presented in order to derive the packet reception rate.

2.1 System Model

In a V2V communication environment, all the vehicles on the road broadcast their data packets with a fixed size to exchange their current states. However, if we focus on one arbitrary vehicle station transmitting the data packet as T-VS, transmissions of the other transmitting vehicle stations that are referred to as interfering vehicle stations (I-VSs) may collide with the T-VS's

---

[*1] When two packets collide, if the power ratio of one packet to the other packet plus the noise is higher than a required Signal-to-Interference-and-Noise power Ratio (SINR) value, the former packet can be successfully received.
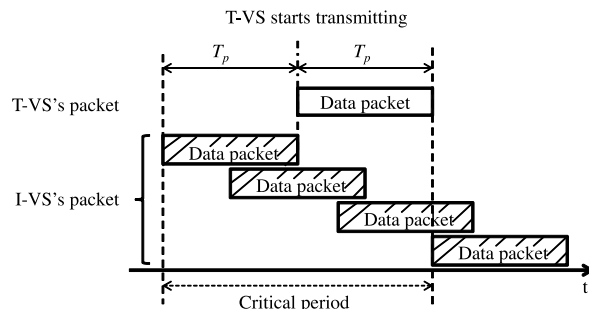
Fig. 2   The critical period for broadcast transmission.
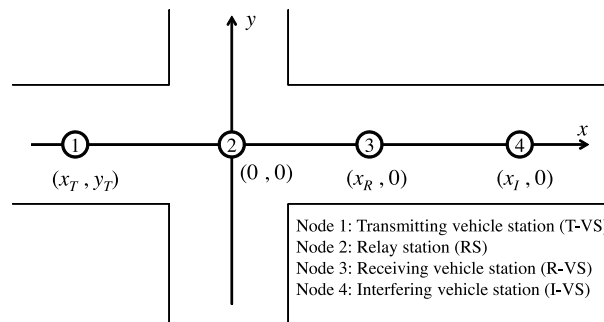
Fig. 3   Nodes layout model for our investigation.

transmission as shown in **Fig. 2**, where T_p represents the duration of transmitting a data packet. Collision only happens during the period that begins T_p seconds before the start of T-VS's transmission and ends with the transmission, which is referred to as *the critical period* or *the vulnerable period* in Ref. [5]. The most probable case is that only one I-VS transmits during the critical period in the vicinity of the T-VS [8] since the critical period is sufficiently shorter than the data generation interval of each vehicle. From this observation, we can introduce a simple model with four nodes distributed around the intersection as illustrated in **Fig. 3**. Node 2 is the RS at the center of the crossroad, where we set the origin of the coordinates. T-VS (Node 1), I-VS (Node 4) and R-VS (Node 3) are placed around the crossroad according to their coordinates. R-VS and I-VS are placed on the x-axis. T-VS can be placed on either the x- or y-axis. In this case, critical interference may happen at the R-VS due to the presence of I-VS.

2.2 Assumptions of the Model

In our analytical model, the V2V broadcast communication with RS is performed based on the following assumptions.

- Both T-VS and I-VS periodically broadcast packets with the same time interval T, which is set large enough to guarantee that the collision only happens in the same time interval. I-VS is supposed to have a packet ready to be broadcasted during the critical period of T-VS. Every packet has the same payload size such as 100 byte and its length T_p is short relative to the coherence time of the fading channel. Thus the received signal power is assumed as unchanged during the period that one packet is either sensed or received. The IEEE 802.11p [9] MAC protocol, a typical CSMA/CA protocol, is employed.

- In broadcast communication, the transmitter is unaware of unsuccessful transmissions. Hence, Automatic Repeat re-

Quest (ARQ) retransmission is not performed and the contention window size W does not increase exponentially.

- The whole broadcast communications basically employ single frequency channel. However, the dedicated frequency band case is also considered for comparison, which employs two frequency bands, one for the direct V2V transmission and the other for the relay transmission.

2.3 Packet Reception Rate

Based on the model and assumptions described above, the packet reception rate of V2V broadcast communication with RS is analyzed.

Let $p_{i,j}^{(CS)}$ denote the probability that node j fails to sense node i's transmission. It can be calculated as the probability that the detected power falls below a chosen threshold during a carrier sense period. Here, the detected power is simplified as the sum of the received signal power and the thermal noise power of that carrier sense period. $p_{i,j}^{(CS)}$ takes the form as

$$p_{i,j}^{(CS)} = p(C_{ij} + N_{CS} < CST), \tag{1}$$

where N_{CS} is the thermal noise power which is simplified as the average during the carrier sense period, considering that the noise power variation has minor impact on carrier sense performance. CST is the carrier sense threshold power. C_{ij} is the received signal power at node j from node i after Rayleigh fading attenuation. The *probability density function* (PDF) of the instantaneous received power over Rayleigh fading is written by

$$f(C_{ij}) = \frac{1}{\sigma_{ij}^2} \exp\left(-\frac{C_{ij}}{\sigma_{ij}^2}\right), \tag{2}$$

where σ_{ij}^2 is the average received power at node j from node i determined by a path loss model.

N_{CS} in Eq. (1) is measured as $N_{CS} = \frac{1}{T_{CS}} \int_0^{T_{CS}} N(t)dt$, where T_{CS} represents the carrier sense period and $N(t)$ is the instantaneous thermal noise power. The PDF of $N(t)$ is given by

$$f(N(t)) = \frac{1}{N} \exp\left(-\frac{N(t)}{N}\right), \tag{3}$$

where N is the average thermal noise power in the receiving band. Note that $N(t)$ and C_{ij} are statistically independent. Since T_{CS} is much longer than the inverse of the noise bandwidth, N_{CS} can be further approximated as N.

Substituting Eq. (2) into Eq. (1) and replace N_{CS} with N, Eq. (1) can be written as

$$p_{i,j}^{(CS)} = \int_0^{CST-N} f(C_{ij})dC_{ij} = 1 - \exp\left(\frac{N-CST}{\sigma_{ij}^2}\right). \tag{4}$$

Let $p_{i,j,m}^{(I)}$ denote the probability that the data packet transmitted from node i is successfully received at node j under the interference from node m. It is calculated as the probability that the received Signal-to-Interference-and-Noise power Ratio (SINR) exceeds the required SINR threshold, which is given by

$$p_{i,j,m}^{(I)} = p\left(\frac{C_{ij}}{C_{mj}+N} \geq \Gamma_{SINR}\right), \tag{5}$$

where Γ_{SINR} is the required SINR threshold to successfully receive the packet. C_{mj} is the instantaneous interference power

from node m at node j. It obeys the same distribution as C_{ij} in Eq. (2). Since C_{ij} and C_{mj} are independent, $p_{i,j,m}^{(I)}$ can be calculated in terms of the distribution functions of C_{ij} and C_{mj} as

$$
\begin{aligned}
p_{i,j,m}^{(I)} &= 1 - \int_0^\infty \int_0^{\Gamma_{SINR}(C_{mj}+N)} f(C_{ij})f(C_{mj})dC_{ij}dC_{mj} \\
&= 1 - \int_0^\infty \int_0^{\Gamma_{SINR}(C_{mj}+N)} \frac{1}{\sigma_{ij}^2} \exp\left(\frac{C_{ij}}{\sigma_{ij}^2}\right) \\
&\quad \cdot \frac{1}{\sigma_{mj}^2} \exp\left(\frac{C_{mj}}{\sigma_{mj}^2}\right)dC_{ij}dC_{mj} \\
&= \frac{\sigma_{ij}^2 \exp\left(\frac{-\Gamma_{SINR}N}{\sigma_{ij}^2}\right)}{\sigma_{ij}^2 + \Gamma_{SINR}\sigma_{mj}^2}.
\end{aligned} \tag{6}
$$

Let $p_{i,j}^{(N)}$ denote the probability of successful reception at node j from node i without any interference from the other node and it is given by

$$
\begin{aligned}
p_{i,j}^{(N)} &= p\left(\frac{C_{ij}}{N} \geq \Gamma_{SINR}\right) \\
&= \exp\left(-\frac{\Gamma_{SINR}N}{\sigma_{ij}^2}\right).
\end{aligned} \tag{7}
$$

From the model shown in Fig. 3, depending on the packet generation orders of Node 1 and Node 4 and the success of carrier sense of transmission from the corresponding node, the interaction of the transmissions from Node 1, Node 2 and Node 4 can be classified into several situations. In the following analysis, all the possible situations are listed, and the packet reception rate as well as the probability of occurrence for each situation are calculated with $p_{i,j}^{(CS)}$, $p_{i,j,m}^{(I)}$ and $p_{i,j}^{(N)}$. Note that single frequency operation is assumed below, unless otherwise specified.

Situation 1: Node 1 has a packet ready to be transmitted slightly earlier than Node 4. The probability of occurrence for this situation is 0.5.

Situation 1.1: As shown in **Fig. 4**, if Node 4 fails to sense the ongoing transmission of Node 1, the two packets will collide at Node 2 and Node 3. However, the packet can still be received successfully because of the capture effect. Under this situation, if Node 2 can receive the packet from Node 1 successfully, it will forward the packet after decoding it on the premise that the channel is sensed as idle for the DCF Interframe Space (DIFS) time interval.

Then Node 3 will receive the relayed packet without interfer-
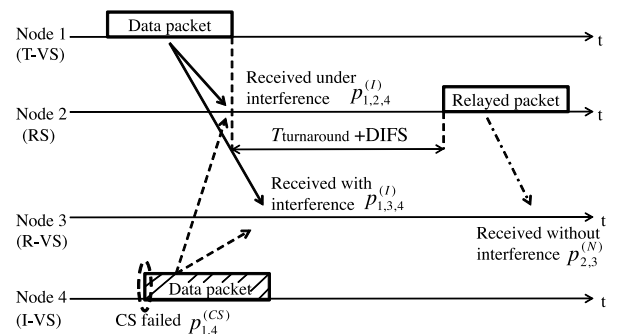
$T_{\text{turnaround}}$ is the RX/TX turn around time necessary for a transceiver hardware to switch between transmission and reception modes.

Fig. 4 Packet transmission in Situation 1.1.

ence. The packet reception rate at R-VS from T-VS in this case which is denoted as $p_{1.1}$ can be represented as

$$p_{1.1} = \frac{1}{2} p_{1,4}^{(CS)} (p_{1,3,4}^{(I)} + (1 - p_{1,3,4}^{(I)}) \, p_{1,2,4}^{(I)} \, p_{2,3}^{(N)}), \tag{8}$$

where $(1 - p_{1,3,4}^{(I)}) \, p_{1,2,4}^{(I)} \, p_{2,3}^{(N)}$ expresses the diversity gain in the packet reception rate obtained from the relayed path.

Dedicated frequency band case for Situation 1.1: The packet reception rate when different frequency bands are assigned for the direct V2V communication and the relay transmission corresponding to Situation 1.1 is the same as the single frequency band case as shown in Eq. (8).

Situation 1.2: If Node 4 senses that the channel is busy, it will postpone its transmission according to the backoff mechanism defined by IEEE 802.11p. According to the mechanism, Node 4 first sets the backoff timer T_b, which can be expressed as

$$T_b = n_b \times \delta, \tag{9}$$

where n_b is an integer randomly chosen within the backoff range $[0, W - 1]$ and δ is the unit slot time.

When the channel becomes idle and the idle state lasts for a DIFS interval, the backoff timer will start to decrement. Node 4 would transmit when the backoff timer reaches zero. Then, Node 1's packet will be received by Node 2 and Node 3 without the interference from Node 4. Nevertheless, there is a chance that Node 4's deferred transmission will overlap with the relay transmission from Node 2.

Situation 1.2.1: If the delayed packet from Node 4 collides with the relayed packet, Node 3 will receive the relayed packet under interference. According to the setting of Node 4's backoff timer, Node 4 can transmit earlier or later than the relay transmission, as shown in **Fig. 5**. In the figure, there are two cases for the order of transmissions. In case 1, Node 4 starts its transmission earlier than Node 2. The condition that Node 4's transmission overlaps with the relay transmission is given by

$$T_{b1} < T_{turnaround} < T_{b1} + T_p, \tag{10}$$

where T_{b1} is the backoff timer for case 1 and $T_{turnaround}$ represents the RX/TX turnaround time.

Let n_1 denote the number of values that satisfy Eq. (10). Assuming $T_{turnaround} < T_p$ and considering Eq. (9), we obtain

$$n_1 = \left\lceil \frac{T_{turnaround}}{\delta} \right\rceil, \tag{11}$$

where $\lceil \, \rceil$ is the round up function. If Node 2 fails to sense the on-going transmission of Node 4, the two packets will collide. The
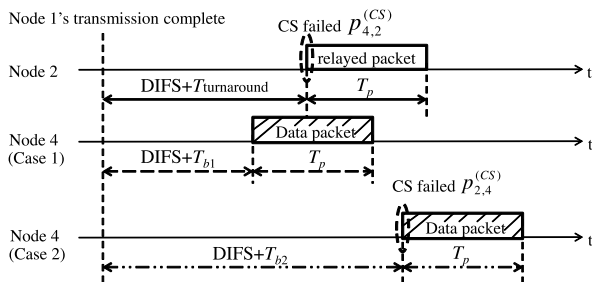
probability of collision in this case is given by

$$p_{c1} = (n_1/W) \times p_{4,2}^{(CS)}. \tag{12}$$

Similarly, in case 2 when the relay transmission precedes Node 4's transmission, if overlapping happens and Node 4 fails to sense the busy channel, the two packets will collide. This probability can be expressed as

$$p_{c2} = (n_2/W) \times p_{2,4}^{(CS)}, \tag{13}$$

$$n_2 = \left\lfloor \frac{T_{turnaround} + T_p}{\delta} \right\rfloor - \left\lfloor \frac{T_{turnaround}}{\delta} \right\rfloor, \tag{14}$$

where n_2 is derived from $T_{turnaround} < T_{b2} < T_{turnaround} + T_p$ and Eq. (9). Note that T_{b2} denotes the backoff timer for case 2, $\lfloor \, \rfloor$ represents the round down function.

Then the packet reception rate under Situation 1.2.1 is

$$p_{1.2.1} = \frac{1}{2}(1 - p_{1,4}^{(CS)})(p_{c1} + p_{c2})(p_{1,3}^{(N)} + (1 - p_{1,3}^{(N)}) \, p_{1,2}^{(N)} \, p_{2,3,4}^{(I)}). \tag{15}$$

Situation 1.2.2: If the duration of Node 4's transmission does not overlap with the relay transmission, or either Node 2 or Node 4 succeeds to sense the busy channel, the relayed packet will be received without collision. The packet reception rate is expressed as

$$p_{1.2.2} = \frac{1}{2}(1 - p_{1,4}^{(CS)})(1 - (p_{c1} + p_{c2})) \\ \cdot (p_{1,3}^{(N)} + (1 - p_{1,3}^{(N)}) \, p_{1,2}^{(N)} \, p_{2,3}^{(N)}). \tag{16}$$

Dedicated frequency band case for Situation 1.2: When different frequency bands are assigned for the direct V2V communication and the relay transmission, the collision between Node 4's transmission and the relay transmission can be avoided. The packet reception rate corresponding to Situation 1.2 is given by

$$p_{1.2}' = \frac{1}{2}(1 - p_{1,4}^{(CS)})(p_{1,3}^{(N)} + (1 - p_{1,3}^{(N)}) \, p_{1,2}^{(N)} \, p_{2,3}^{(N)}). \tag{17}$$

Situation 2: Node 1 generates the packet slightly later than Node 4. The probability of occurrence for this situation is also 0.5.

Situation 2.1: Similar to Situation 1.1, if Node 1 fails to sense Node 4's transmission, Node 1's packet and Node 4's packet will collide at Node 2 and Node 3. The relay transmission will complete without interference if Node 2 receives the packet from Node 1 successfully. The packet reception rate from Node 1 to Node 3 in this case is

$$p_{2.1} = \frac{1}{2} p_{4,1}^{(CS)} (p_{1,3,4}^{(I)} + (1 - p_{1,3,4}^{(I)}) \, p_{1,2,4}^{(I)} \, p_{2,3}^{(N)}). \tag{18}$$

Dedicated frequency band case for Situation 2.1: The packet reception rate for the dedicated frequency band case corresponding to Situation 2.1 is the same as the single frequency band case as shown in Eq. (18).

Situation 2.2: If Node 1 senses that the channel is busy due to Node 4's transmission, it will postpone its transmission according to the backoff mechanism. Then, Node 1's deferred transmission might overlap with the relayed transmission from Node 2, which originates from Node 4.

Fig. 5 Collision timing of transmissions from Node 4 and Node 2 when Node 4 transmits earlier.

Situation 2.2.1: If Node 1's transmission overlaps with Node 2's transmission, Node 2 cannot forward the packet transmitted from Node 1 due to the receive failure.

Similar to Situation 1.2.1, the probability of collision is given by

$$p_{c3} = (n_1/W) \times p_{1,2}^{(CS)} + (n_2/W) \times p_{2,1}^{(CS)}. \quad (19)$$

Under this situation, the packet reception rate from the T-VS to the R-VS is given by

$$p_{2.2.1} = \frac{1}{2}(1 - p_{4,1}^{(CS)}) \, p_{c3} \, p_{1,3,2}^{(I)}. \quad (20)$$

Situation 2.2.2: Similar to Situation 1.2.2, if Node 1's packet does not collide with the relayed packet, the packet reception rate is expressed as

$$p_{2.2.2} = \frac{1}{2}(1 - p_{4,1}^{(CS)})(1 - p_{c3})(p_{1,3}^{(N)} + (1 - p_{1,3}^{(N)}) \, p_{1,2}^{(N)} \, p_{2,3}^{(N)}). \quad (21)$$

Dedicated frequency band case for Situation 2.2: Direct V2V transmission and relay transmission are free of interference. The packet reception rate from T-VS to R-VS corresponding to Situation 2.2 is

$$p'_{2.2} = \frac{1}{2}(1 - p_{4,1}^{(CS)})(p_{1,3}^{(N)} + (1 - p_{1,3}^{(N)}) \, p_{1,2}^{(N)} \, p_{2,3}^{(N)}). \quad (22)$$

Finally, the packet reception rate from T-VS to R-VS is the sum of the successful transmission probabilities corresponding to the above situations, which is given by

$$p = p_{1.1} + p_{1.2.1} + p_{1.2.2} + p_{2.1} + p_{2.2.1} + p_{2.2.2}. \quad (23)$$

The packet reception rate when dedicated frequency bands are assigned for direct V2V communication and relay transmission is

$$p' = p_{1.1} + p'_{1.2} + p_{2.1} + p'_{2.2}. \quad (24)$$

3. Numerical Results

In this section, we apply the proposed model described in Section 2 to a specific intersection scenario. The analytical results and simulation results are presented in LOS environment (Section 3.1) and NLOS environment (Section 3.2). We will confirm the proposed analytical model via simulations and discuss the impact of location of nodes, hidden terminal, carrier sensitivity and RF frequency band.

In order to validate the proposed model, we obtained the packet reception rates of the IEEE 802.11p CSMA/CA broadcast relay network by a series of simulations using a network simulator (QualNet 4.5 [10]). For the accuracy of simulations, each simulation round lasts 1,000 seconds and results are averaged over 10 independent runs.

We implemented the IEEE 802.11p standard in QualNet, which is basically extended from the 802.11a implementation. The original capture algorithm in QualNet is implemented in such a way that when two signals arrive at a receiver, the receiver only accepts the stronger signal that arrives earlier than the other one. However, current wireless receivers accept the stronger signal even if it arrives after the other one [11]. Therefore, the capture

Table 1 Physical and MAC parameters for theoretical model and simulation.

RF frequency	5.9 GHz, 700 MHz
Transmission Power	18 dBm
VS antenna height	1.5 m
RS antenna height	6 m
Street width	10 m
Pathloss model	ITU-R P.1411-5
Fading model	Rayleigh
Maximum Doppler frequency	196.7 Hz/5.9 GHz 23.3 Hz/700 MHz
Data rate/Modulation	6 Mbps/QPSK
Contention window size W	32
Slot time δ	13 μs
DIFS	58 μs
$T_{turnaround}$	2 μs
Carrier sense threshold CST	−80 dBm, −85 dBm, −90 dBm
SINR threshold Γ_{SINR}	10
Noise factor	10

Table 2 Traffic condition and configurations of simulation.

Packet type	UDP broadcast
Packet payload size	100 byte
Packet generation interval	100 ms
Start time	(0, 264 μs)
Duration of simulation	1,000 s

algorithm in QualNet is modified to accept the strongest signal no matter its arrival order.

The configurations and parameters used in the analytical model and in the simulations are summarized in **Table 1**. The propagation environment is characterized by the ITU-R P.1411-5 path loss model [12] which models both LOS and NLOS propagation loss under the influence of shadowing caused by buildings around the intersection. The maximum Doppler frequency is set corresponding to the vehicle's speed of 36 km/h. For the traffic configuration in the simulations, the traffic generator (*Traffic-Gen*) which broadcasts UDP packets with a fixed payload size (100 byte) and interval (100 ms) is employed, as shown in **Table 2**. Given the conditions in Table 1, the duration of each packet T_p is 264 μs, which determines the upper bound of transmission start time for T-VS and I-VS shown in Table 2.

3.1 LOS Environment

Set the y coordinates of T-VS, R-VS and I-VS as zero ($y_T = y_R = y_I = 0$), as shown in Fig. 3. The value of x_R is assigned with values from 0 m to 300 m with a 10 m step, and x_I varies from −300 m to 300 m with a 20 m step. The value of x_T is fixed at −50 m. Carrier sense threshold CST varies from −80 dBm to −90 dBm with a 5 dB step.

The packet reception rates for 5.9 GHz obtained by theoretical calculation and simulation with different CSTs are shown in **Fig. 6** (a) and Fig. 6 (b), respectively. Comparing these two figures, we can see that the theoretical calculation well describes the characteristics of the packet reception ratio with various locations of R-VS and I-VS and different values of carrier sense threshold. The average differences of the packet reception rates between the simulations and the numerical results are less than 1% for all CSTs. Therefore it is concluded that the results obtained by the analytical model can well express the packet recep-
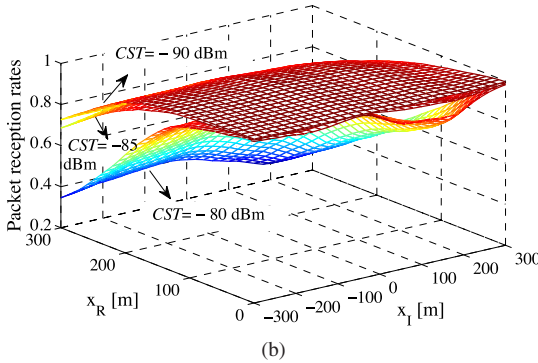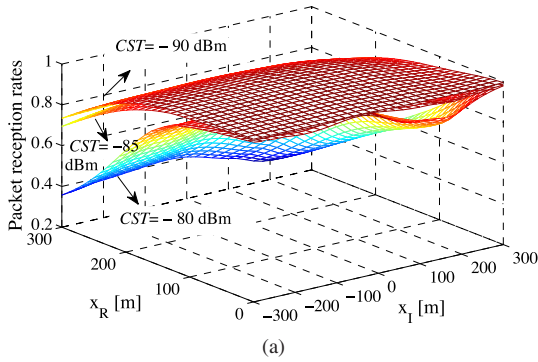
Fig. 6 LOS packet reception rates for different *CST* obtained by (a) theoretical calculation and (b) simulations with 5.9 GHz band.
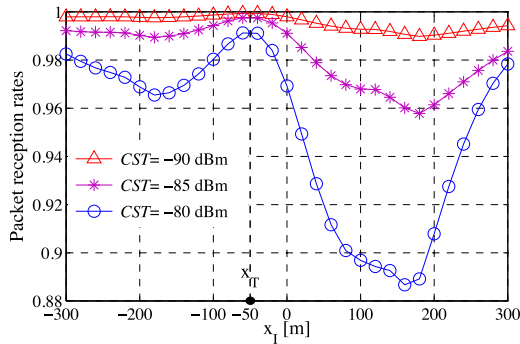
Fig. 7 LOS packet reception rates for different *CST* with 5.9 GHz band when x_R is 0 m.

Fig. 8 LOS packet reception rates for different x_T with 5.9 GHz band.
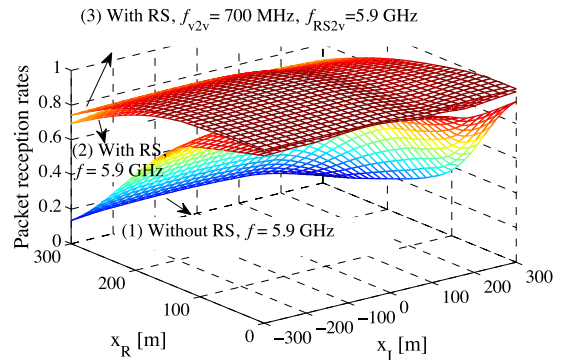
Fig. 9 LOS packet reception rates for different schemes: (1) direct V2V communication without RS, (2) relayed communication with a single frequency band, and (3) relayed communication with two frequency bands.

tion rate performance.

It is also observed that when the carrier sense threshold increases, the packet reception rates degrade (about 3.4% on average when *CST* increases from −90 dBm to −85 dBm and 17.0% when *CST* varies from −85 dBm to −80 dBm), and the magnitude of fluctuation becomes larger. This is because higher carrier sensitivity alleviates the impact of the hidden terminal problem. However, it does not mean that higher carrier sensitivity is always better. If the carrier sense threshold is close to the thermal noise level, the channel will be frequently sensed as busy even if there is no ongoing transmission. From the performance shown in Fig. 6 (a) and Fig. 6 (b), it is clear that −85 dBm is an appropriate choice for the carrier sense threshold.

Figure 7 shows a case when x_R is fixed at 0 m and x_I varies from −300 m to 300 m. It can be observed that the tendencies of these three curves are the same, having a ridge and two valleys, while their depths are different. The highest packet reception rates are obtained when I-VS and T-VS are located at the same position, which results in perfect carrier sense. The reason for the degradation is that when the distances of I-VS from T-VS and RS increase, the probability of collision increases because physical carrier sense cannot work well due to high path loss and fading attenuation. However, if the distance further increases and the average received power at R-VS from I-VS decrease sufficiently, it cannot block the reception of T-VS's packet at R-VS. Therefore two valleys appear in the figure.

With 5.9 GHz band and a *CST* of −85 dBm, the influence of different locations of T-VS (x_T) on the packet reception rates is shown in **Fig. 8**. Increasing x_T makes the performance deteriorate in all ranges of x_R and x_I. This is due to the fact that the averaged received power at R-VS and RS both decreases as x_T increases, which reduce the packet reception rates of direct V2V transmission and relay transmission. Therefore, the location of RS has significant influence on the performance. In order to achieve high packet reception rates, RS should be placed close to T-VS.

Figure 9 shows the improvement in the packet reception rates when RS is used for a *CST* of −85 dBm. With the assistance of RS to obtain path diversity gain, the maximum improvement is up to 58.7% with single 5.9 GHz band. Further improvement (69.5%) is observed when the frequency combination of 700 MHz for direct V2V communication and 5.9 GHz for relay transmission is applied. The latter scheme avoids collision between direct V2V communication and relay transmission. It also improves the packet reception rates and extends carrier sense range in direct V2V communication by using 700 MHz band that has lower propagation loss than 5.9 GHz band.
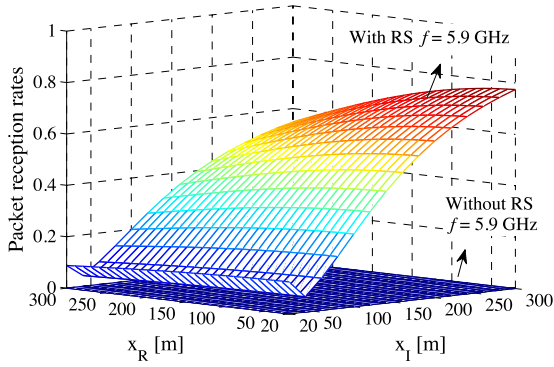
Fig. 10 NLOS packet reception rates for direct V2V communication and broadcast relay communication with 5.9 GHz band.
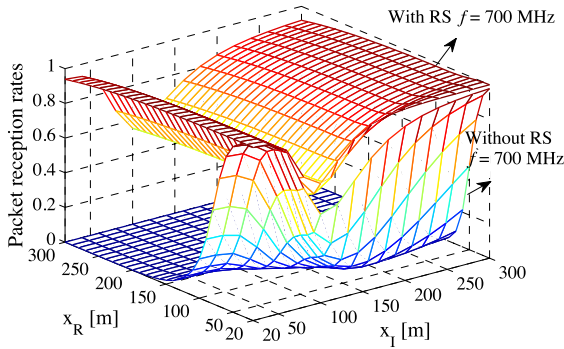
Fig. 11 NLOS packet reception rates for direct V2V communication and broadcast relay communication with 700 MHz band.

3.2 NLOS Environment

In the following analysis, T-VS (Node 1) is located on the south street with x_T set as 0 m and y_T fixed as -50 m, while R-VS (Node 3) is located on the east street with y_R set as 0 m and x_R varies from 20 m to 300 m with a 10 m step (since NLOS propagation loss formula has much error when $x_R < 20$ m). The buildings on the corner may block the LOS path between T-VS and R-VS. I-VS is located on the west/east street with y_I set as 0 m and x_I which varies from 20 m to 300 m with a 20 m step. Carrier sense threshold *CST* is set as -85 dBm.

Figure 10 shows the packet reception rates in the NLOS environment with 5.9 GHz band. It is found that direct V2V communication with 5.9 GHz band suffers from severe propagation loss, and it is almost impossible to deliver a packet from T-VS to R-VS. With the assistance of RS, the performance is improved significantly for large x_I. However, when x_I is small, the interference from I-VS becomes noticeable, which makes RS difficult to receive the packet from T-VS, and the packet reception rate degrades.

The packet reception rates in NLOS environment when 700 MHz band is applied is depicted in **Fig. 11**. Since 700 MHz has a lower diffraction loss and propagation loss than 5.9 GHz band [13], it shows wider communication range both with and without RS, compared with Fig. 10. In addition, the gap between the lowest and the highest packet reception rates for the same x_R with 700 MHz band is smaller than that with 5.9 GHz band. Since the gap is mainly caused by unsuccessful reception at RS from T-VS due to the hidden terminal problem, this observation indicates that a lower frequency band could ease the hidden terminal problem for the broadcast relay network in the NLOS environment.
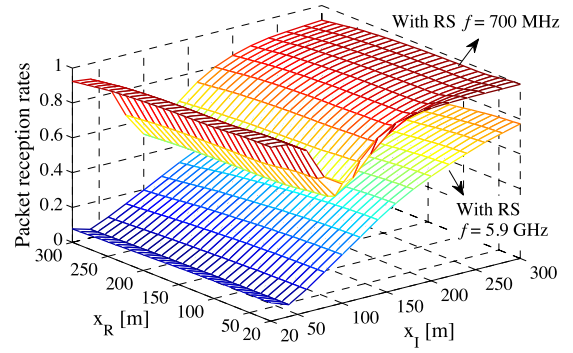
Fig. 12 NLOS packet reception rates obtained by simulation for 5.9 GHz and 700 MHz bands with a RS.
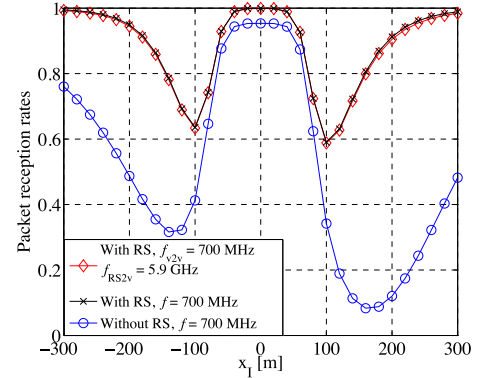
Fig. 13 NLOS packet reception rates for direct V2V communication and broadcast relay communication with a single 700 MHz band and dual frequency bands ($x_R = 50$ m).

Figure 12 depicts the packet reception rates obtained by the simulations in the NLOS environment for 5.9 GHz and 700 MHz bands with RS. Comparing this figure with Figs. 10 and 11, the packet reception rates obtained from simulations and the analytical model match very well (the average differences are 0.8% for 5.9 GHz and 0.83% for 700 MHz), which validates the accuracy of our analytical model for NLOS environment.

In order to investigate whether there is an influence of the symmetric movement of I-VS, the performance results are presented when R-VS is located on the east street with (x_R, y_R) as (50 m, 0 m) and I-VS is located on the west/east street with y_I set as 0 m and x_I from -300 m to 300 m with a 20 m step, as shown in **Fig. 13**. From the figure, it can be seen that all the three curves are "W"-shaped, while their magnitudes of fluctuation are different. The reason for such a shape is the same as for the LOS case. Although the curve of the packet reception rates without RS is asymmetric to x_I, the degrees of the asymmetry of the packet reception rates are decreased with the usage of RS. The reasoning of the weak asymmetry is as follows. The packet reception rates given by Eq. (23) or Eq. (24) are the sum of several terms corresponding to different situations explained in Section 2.3. For Situation 1.1, the two terms $\frac{1}{2}p_{1,4}^{(CS)} p_{1,3,4}^{(I)}$ and $\frac{1}{2}p_{1,4}^{(CS)}(1 - p_{1,3,4}^{(I)}) p_{1,2,4}^{(I)} p_{2,3}^{(N)}$ in Eq. (8) are asymmetric to x_I due to the asymmetry of $p_{1,3,4}^{(I)}$ and $p_{1,2,4}^{(I)}$. However, the sum of the two terms becomes almost symmetric as shown in **Fig. 14**. Similarly, the packet reception rates for Situation 2.1 are almost symmetric. Situations 1.2.1 and 2.2.1 rarely happen because RS can well sense I-VS or T-VS with its higher antenna height and favorable location to get LOS path to
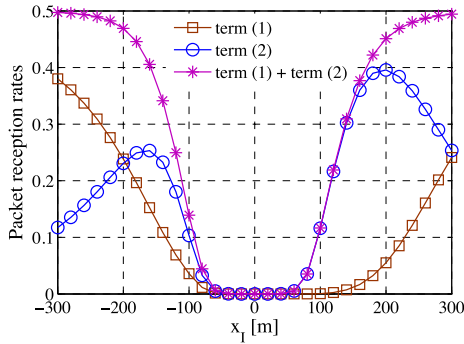
Fig. 14 Probabilities in Eq. (8) for 700 MHz band for the NLOS case with $x_R = 50$ m (term (1) $\frac{1}{2}p_{1,4}^{(CS)}p_{1,3,4}^{(I)}$, term (2) $\frac{1}{2}p_{1,4}^{(CS)}(1 - p_{1,3,4}^{(I)})p_{1,2,4}^{(I)}p_{2,3}^{(N)}$).

all vehicle stations. For the other situations, the packet reception rates, $p_{1.2.2}$ (Eq. (16)), $p_{2.2.2}$ (Eq. (21)), $p'_{1.2}$ (Eq. (17)), $p'_{2.2}$ (Eq. (22)), are symmetric to x_I. Therefore, the packet reception rates of applying RS result in almost symmetric to x_I in the NLOS environment, in contrast to the obviously asymmetric result for the LOS case shown in Fig. 7.

In Fig. 13, it is also observed that the performance is improved when RS is applied to obtain path diversity. The maximum improvement is up to 80% when x_I is 200 m. Although the collisions between direct V2V communication and relay transmission are avoided by allocating two frequency bands for them, there is hardly any improvement observed between the packet reception rate with two frequency bands than that with 700 MHz alone. It is because the collisions between direct V2V communication and relay transmission barely happen due to the sufficient carrier sense performance of RS, as mentioned above.

4. Conclusion

In this paper, an analytical model was proposed to evaluate the packet reception rate performance of a CSMA/CA based broadcast communication using a roadside RS. The model considered the impact of the fading environment, hidden terminal and the capture effect. The network simulation results justified the accuracy of the proposed model. From the analysis of the broadcast network with RS on the intersection, we can observe the following:

- In the NLOS environment, due to severe diffraction loss, direct V2V communication with 5.9 GHz band hardly delivers packets from T-VS to R-VS, whereas direct V2V communication with 700 MHz band performs better up to a range of 150 m from the center of the intersection.
- The communication range can be extended with a RS. The coverage can be extended to more than 300 m with 700 MHz band if we accept the packet reception rate of 60%.
- Packet reception rate performance can be improved by applying RS to obtain path diversity gain, and the degree of improvement is influenced by the location of the RS. In general, higher improvement can be obtained if RS is located closer to the T-VS. Nevertheless, even if the RS is positioned very close to the T-VS, significant improvement is not guaranteed due to the hidden terminal problem which blocks the reception from T-VS at RS.

- Broadcast V2V communication suffers from the hidden terminal problem, which can be alleviated by increasing carrier sensitivity. However, as mentioned before, too high carrier sensitivity would result in unnecessary delay of transmission. Since the occurrence of the hidden terminal problem also depends on the detected power, an alternative way is to increase received signal power by employing a lower frequency band which has a lower path loss. To mitigate the hidden terminal problem, a carrier sense threshold of -85 dBm and RF frequency of 700 MHz is recommended.

The proposed model revealed the influence of the path diversity effect, the positions of nodes, the carrier sense threshold and the RF frequency band on the performance of the CSMA/CA based broadcast relay network in a vehicular environment. It provides references for selections and optimization of systems parameters to achieve high reliability of vehicular networks. In this paper, one I-VS was considered in the analytical model. When there are multiple I-VSs transmitting during the critical period of T-VS, packet collisions between data packets and relayed packets will occur more frequently and the performance might deteriorate. The theoretical performance analysis with multiple I-VSs remains a future work.

References

[1] Chen, W. and Cai, S.: Ad hoc peer-to-peer network architecture for vehicle safety communications, *Communications Magazine*, Vol.43, No.4, pp.100–107, IEEE (2005).

[2] Yamao, Y. and Minato, K.: Vehicle-roadside-vehicle relay communication network employing multiple frequencies and routing function, *Proc. IEEE ISWCS2009*, Siena, Italy, pp.413–417 (2009).

[3] Minato, K., Cheng, H. and Yamao, Y.: Performance of Broadcast Transmission from Multiple Vehicles in Vehicle-Roadside-Vehicle Relay Network, *Proc. ChinaCom 2011*, Harbin, China (2011).

[4] Moreno, M.T., Corroy, S., Eisenlohr, F.S. and Hartenstein, H.: IEEE 802.11-based one-hop broadcast communications: Understanding transmission success and failure under different radio propagation environments, *Proc. MSWiM '06*, pp.68–77, ACM (2006).

[5] Ma, X., Chen, X. and Refai, H.H.: On the Broadcast Packet Reception Rates in One-Dimensional MANETs, *Proc. IEEE GLOBECOM 2008*, pp.1–5 (2008).

[6] Ma, X., Chen, X. and Refai, H.H.: Performance and reliability of DSRC vehicular safety communication: A formal analysis, *EURASIP J. Wirel. Commun. Netw.*, Vol.2009, pp.1–13 (2009).

[7] Campolo, C., Vinel, A., Molinaro, A. and Koucheryavy, Y.: Modeling Broadcasting in IEEE 802.11p/WAVE Vehicular Networks, *Communications Letters*, Vol.15, No.2, pp.199–201, IEEE (2011).

[8] Minato, K., Dai, J. and Yamao, Y.: Theoretical Analysis of Broadcast Packet Delivery Rate in ITS V2V Communication with CSMA/CA, *Proc. IEEE VTC Fall 2011*, pp.1–5 (2011).

[9] Jiang, D. and Delgrossi, L.: IEEE 802.11p: Towards an International Standard for Wireless Access in Vehicular Environments, *Proc. IEEE VTC Spring 2008*, pp.2036–2040 (2008).

[10] Scalable Network Technologies, Inc.: Qualnet Simulator, Version 4.5, available from ⟨http://www.scalable-networks.com⟩.

[11] Kochut, A., Vasan, A., Shankar, A.U. and Agrawala, A.: Sniffing out the correct physical layer capture model in 802.11b, *Proc. ICNP 2004*, pp.252–261 (2004).

[12] Recommendation ITU-R P.1411-5: Propagation data and prediction methods for the planning of short-range outdoor radiocommunication systems and radio local area networks in the frequency range 300 MHz to 100 GHz (2009). International Telecommunication Union.

[13] Iwai, H., Tango, T., Murakami, Y., Sasaki, K. and Horomatsu, T.: On Frequency Dependence of Propagation in Non Line-of-Sight V2V Communications, *Proc. 15th World Congress on ITS 2008*, New York, USA (2008).

Huiting Cheng received her B.S. degree in wireless communications from Harbin Engineering University, China, in 2008 and her M.S. degree from University of Southampton, UK, in 2009. Since October of 2010, she has been working towards her Ph.D. degree in information and communication engineering at the University of Electro-Communications, Tokyo, Japan.

Yasushi Yamao received his B.S. M.S. and Ph.D. degrees in electronics engineering from Kyoto University, Kyoto, Japan, in 1977, 1979, and 1998, respectively. He started his research career of mobile communications from the measurement and analysis of urban radio propagation as his M.S. thesis. In 1979, he joined the Nippon Telegraph and Telephone Corporation (NTT) Laboratories, Japan, where his major activities included leading research on GMSK modulator/demodulator and GaAs RF ICs for digital mobile communications, and the development of PDC digital cellular handheld phones. In 1993, he moved to NTT DoCoMo Inc. and directed the standardization of high-speed paging system (FLEX-TD) and the development of 3G radio network system. He also joined European IST research programs for IP-based 4th generation mobile communication. In 2005, he moved to the University of Electro-Communications as a professor of the Advanced Wireless Communication Research Center (AWCC). His current interests focus on wireless ubiquitous communication networks and protocols, as well as high-efficiency and reconfigurable wireless circuit technologies both in RF and Digital Signal Processing. He is a Fellow of IEICE and a member of IEEE. He served as Vice President of IEICE Communications Society (2003–2004), Chairman of the IEICE Technical Group on Radio Communication Systems (2006–2008) and Chief Editor of IEICE Communication Magazine (2008–2010). He is currently Vice Chairman of the IEEE VTS Japan Chapter.